Size-controlled quantum dots fabricated by precipitation of epitaxially grown, immiscible semiconductor heterosystems

2008 J. Phys.: Condens. Matter 20 454216

(http://iopscience.iop.org/0953-8984/20/45/454216)

J. Phys.: Condens. Matter **20** (2008) 454216 (4pp) doi:10.1088/0953-8984/20/45/454216

Size-controlled quantum dots fabricated by precipitation of epitaxially grown, immiscible semiconductor heterosystems

H Groiss[1], E Kaufmann[1], G Springholz[1], T Schwarzl[1], G Hesser[1], F Schäffler[1], W Heiss[1], K Koike[2], T Ikatura[2], T Hotei[2], M Yano[2] and T Wojtowicz[3]

[1] Institut für Halbleiter und Festkörperphysik, Johannes Kepler Universität, 4040 Linz, Austria
[2] Osaka Institute of Technology, Asahi-ku Ohmiya, Osaka 535-8585, Japan
[3] Institute of Physics, Polish Academy of Sciences, Lotnikov 32/46, 02-668 Warsaw, Poland

Received 11 June 2008
Published 23 October 2008
Online at stacks.iop.org/JPhysCM/20/454216

Abstract

Epitaxial quantum dots with symmetric and highly faceted shapes are fabricated by thermal annealing of two-dimensional (2D) PbTe epilayers embedded in a CdTe matrix. This novel self-organization scheme is based on the immiscibility of the involved semiconductor materials, which originates from the different bulk bonding configurations and the concomitant lattice-type mismatch. By varying the thickness of the initial 2D layers, the dot size can be controlled in a range between 5 and 25 nm, with areal densities as high as 3×10^{11} cm^{-2}. Control of the quantum dot size allows for photoluminescence tuning over a spectral range between 2.2 and 3.7 μm. Multilayer quantum dot stacks with systematically varying sizes yield ultra-broadband emission, and thus a precondition for the development of superluminescence diodes operating in the near- and mid-infrared.

Intense investigations of the unique optical and electronic properties of semiconductor nanocrystals [1] and quantum dots [2, 3] have led to applications such as high-efficiency lasers [4, 5], single-photon sources [6, 7] and other advanced optoelectronic [8, 9] and spintronic [10] devices. As yet, efficient fabrication is based on two self-organization schemes, namely chemical synthesis in a core–shell process [11, 12] and strain-driven three-dimensional island growth of two materials with different lattice constants (Stranski–Krastanov growth) [13, 14]. Both techniques have distinct disadvantages: in the former the organic shell impedes carrier injection, whereas the latter leads to highly asymmetric and often heavily alloyed nanocrystals [15].

Here we demonstrate a different approach that yields almost perfect, size-controllable quantum dots in a single-crystalline matrix without most of the drawbacks of the conventional methods. It is based on non-equilibrium heteroepitaxial growth of two immiscible materials, which decompose into coherently embedded nanocrystals upon annealing. The most widely studied heterosystems of this type consist of the semimetal ErAs, which crystallizes in the rock-salt (*rs*) structure, and the zincblende (*zb*) semiconductors GaAs or $In_{1-x}Ga_xAs$ [16, 17]. Several applications for such semimetal/semiconductor heterostructures are under investigation: they are, however, unsuited for the implementation of quantum dots because of the vanishing bandgap of ErAs. This limitation is overcome by combining the narrow-gap IV–V semiconductor PbTe with the wide-gap II–VI semiconductor CdTe, which differ in their bandgaps by 1.2 eV. The two materials have almost identical lattice constants, but different bonding configurations: PbTe has a fully occupied s-shell and thus forms ionic p-type bonding orbitals. Each atom has six nearest neighbors which define a cubic *rs* lattice. CdTe develops sp^3 hybrid orbitals, which cause crystallization in the fourfold-coordinated *zb* lattice. This lattice-type mismatch results in a large miscibility gap [18], and thus in phase separation near thermodynamic equilibrium. Nevertheless, the two materials can be grown pseudomorphically as two-dimensionally (2D) layered heterostructures by low-temperature molecular beam epitaxy (MBE) [19]. After annealing, the PbTe layer(s) disintegrate into highly symmetric, coherent and defect-free quantum dots with the shape of a *rhombicuboctahedron*. The quantum dots show strongly enhanced photoluminescence as compared to bulk PbTe [20], which is attributed to the

enhanced overlap of the electron–hole-pair wavefunctions in the quantum dots.

The structures were grown by solid-source molecular beam epitaxy (MBE) onto (001) oriented CdTe/GaAs hybrid substrates consisting of one to several micrometers thick CdTe buffer layers on GaAs(001) substrates. The high-quality buffer layers exhibit near-band-edge luminescence only and smooth surfaces with less than 0.5 nm root-mean-square roughness. Subsequently, single or multiple PbTe epilayers were deposited on the Cd-stabilized buffer at 240–250 °C. In this temperature range PbTe and CdTe are virtually lattice-matched, with respective lattice constants of 6.490 and 6.478 Å at 240 °C. The relatively low growth temperature leads to perfectly streaked reflection high-energy electron diffraction (RHEED) patterns throughout the whole deposition process.

To transform the 2D PbTe layers into nanocrystals, the as-grown structures were post-growth annealed at temperatures between 300 and 360 °C for 10 min either *in situ* or in an inert gas atmosphere. The results were investigated by transmission electron microscopy (TEM) with a JEOL 2011 FasTEM instrument operated at 200 keV along the [$\bar{1}$10] and [001] zone axes. Figure 1(a) shows a cross-sectional bright-field image, where the PbTe regions appear darker than the surrounding CdTe matrix. PbTe maintains its *rs* lattice, as confirmed by high-resolution lattice images (figure 1(b)). Because of the different selection rules for diffraction at *rs* and *zb* lattices, only the {111} lattice planes are resolved in the *zb* lattice regions, whereas (002) and (220) lattice planes appear in the *rs* regions. The high-resolution cross-sectional TEM (HRXTEM) image in figure 1(b) shows the marked region of a PbTe quantum dot in figure 1(a), which contains all three terminating faces of a rhombicuboctahedron, namely {100} (lower interface), {110} (left interface) and {111} (inclined interface). To identify the atomic positions of the Cd, Pb and Te atoms, multislice simulations were performed with the commercial JEMS code. A simulated image is depicted in figure 1(c) and the corresponding bulk positions of the atoms are shown in figure 1(d).

More detailed investigations of the atomic configurations at the {100} and {110} interfaces revealed significant (up to 10% of the lattice constant) shifts of the interface atoms from their respective ideal bulk positions [21]. This is a consequence of total energy minimization of the system near interfaces with severe bond-type misfits, and was found to be in excellent quantitative agreement with predictions from *ab initio* calculations [21].

Minimization of the interface energy, and thus of the interface area, is also the main mechanism for the disintegration of an epitaxially defined 2D PbTe layer into quantum dots. Comparing the interface area of a film of thickness d with the surface area of approximately spherical quantum dots of radius r leads to a critical radius $r_c = 3/2d$, above which it becomes energetically favorable for the film to break apart into quantum dots. This means that, for a given film thickness d, there is a lower limit for the radius of the precipitates which is directly proportional to d. One can therefore expect a correlation between the average dot size after annealing and the thickness of the deposited epilayer.

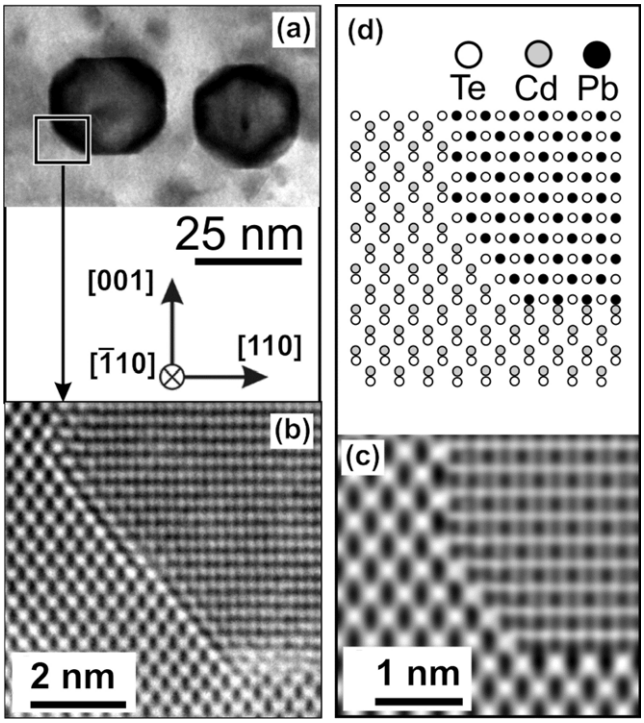

Figure 1. PbTe precipitates in a CdTe matrix fabricated by annealing of 2D PbTe epilayers clad in CdTe. (a) TEM bright-field image of two PbTe quantum dots. (b) HRXTEM image of the marked area in (a), revealing the different lattice types and all three interfaces occurring on the rhomboedrical cubo-octahedron shape of the precipitates. (c) Multislice simulations of the image in (b), with the corresponding positions of the atoms displayed in (d).

Since epilayer thicknesses can be extremely well controlled by MBE, size manipulation of the PbTe precipitates should become feasible.

To demonstrate epitaxial dot size control, we grew a multilayer structure with four PbTe layers of thicknesses 1, 2, 5 and 10 nm that were separated by 50 nm thick CdTe spacer layers. After 2D growth and capping, the sample was annealed *in situ* for 10 min at 360 °C. This converts the 2D layers laterally into well-separated PbTe quantum dots, which remain along the growth direction located in the planes predefined by the original epilayers. An additional set of samples was grown for plan-view TEM and photoluminescence measurements, each containing a single PbTe layer with thicknesses of 1, 3 and 10 nm, respectively. These were post-growth annealed at a somewhat lower temperature of 320 °C.

As expected, increasing thickness of the initial PbTe layers results in increasing size of the PbTe precipitates. This is demonstrated by the dark-field cross-sectional TEM image of the multilayer sample in figure 2. In addition, figure 3 shows to scale cross-sectional and plan-view TEM images of the two reference samples with single PbTe layers of 1 and 3 nm, respectively. The plan-view images clearly show that, with increasing layer thickness, the PbTe precipitates become more and more elongated within the plane of the original epilayer.

To quantify the size and shape of the PbTe precipitates as a function of the epilayer thickness, dot height and width were statistically analyzed employing more than 150 dots from the

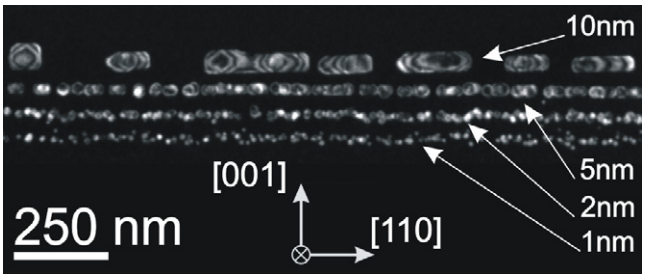

Figure 2. Dark-field cross-sectional TEM image of a PbTe/CdTe multilayer sample containing four PbTe epilayers with 1, 2, 5 and 10 nm thicknesses after 10 min post-growth annealing at 360 °C.

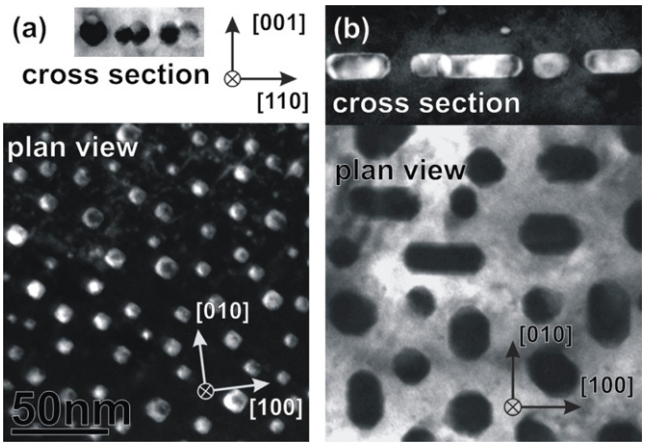

Figure 3. Cross-sectional (top) and plan-view (bottom) TEM images of PbTe epilayers with (a) 1 nm and (b) 3 nm thickness, after annealing at 320 °C for 10 min. All images are to scale.

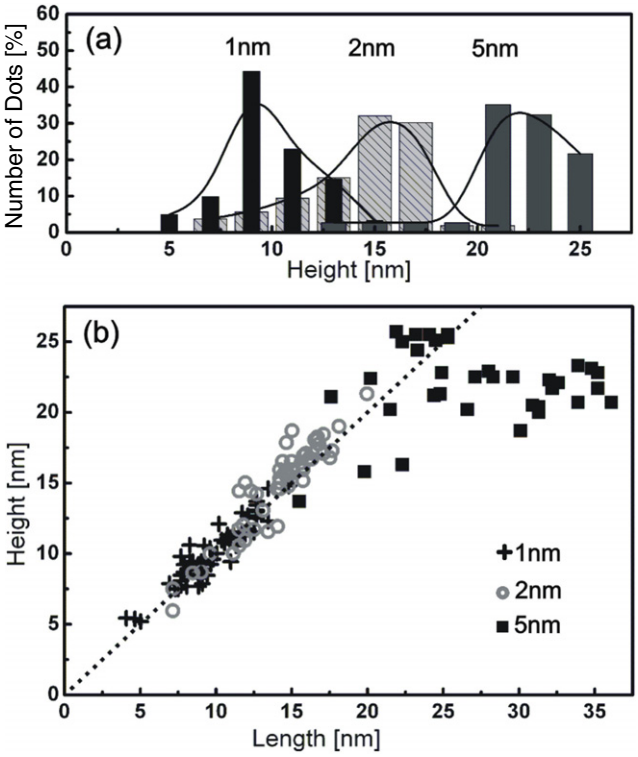

Figure 4. (a) PbTe dot height histograms for the 1, 2 and 5 nm layers of the multilayer sample of figure 2. (b) Corresponding height versus width of the dots. The dotted line represents an aspect ratio of 1.

lower three layers of the TEM image in figure 2. The resulting dot height histograms are displayed in figure 4(a). The lowest 1 nm thick PbTe epilayer was converted by annealing into quantum dots with a height-to-width aspect ratio close to 1 and sizes between 5 and 15 nm, with an average value of 10 nm. (figure 4(b)). The PbTe dots formed from the originally 2 and 5 nm thick layers are considerably larger with average sizes around 14 and 22 nm, respectively. The relative standard variation decreases from ±20% for the 1 and 2 nm layers to ±14% for the 5 nm layer, i.e. the height uniformity of the dots improves with increasing dot size.

With increasing thickness of the initial PbTe layer the shape of the quantum dots changes from the highly symmetric cubo-octahedral shape with aspect ratio of one to precipitates that are still terminated by the same interfaces, but become elongated in the plane of the original epilayer (cf plan-view image in figure 3(b)). This finding indicates that the larger dots have not yet reached their equilibrium shape during annealing. The increasing shape asymmetry is quantified in figure 4(b), where the larger dots from the 5 nm thick epilayer deviate significantly from the dotted line, which marks the height-to-width aspect ratio of one, whereas the thinner layers are essentially symmetric. The shape anisotropy is even more apparent for the 10 nm thick epilayer, which has obviously just started to disintegrate into isolated patches of PbTe regions (figure 2). The shape asymmetry of the larger dots is attributed to the substantial increase of material transport required for the disintegration of the thicker epilayers.

A particularly striking feature of the PbTe nanocrystals is their intense photoluminescence emission at room temperature. For these investigations, the samples were excited with a continuous wave 1480 nm diode laser emitting with a maximum power of 245 mW. The room temperature emission spectrum was recorded by a liquid-nitrogen-cooled InSb infrared detector mounted on a grating spectrometer. The complete set-up was kept under an N_2 atmosphere to reduce mid-infrared atmospheric absorptions. Still, residual water absorption in the optical path leads to a measurement artifact which shows as a dip in the luminescence spectra around 2.6 μm. This range is marked in figure 5 as a shaded area.

The control of the nanocrystal sizes allows for efficient tuning of the photoluminescence properties. This is demonstrated by the room temperature luminescence spectra in figure 5. For the initially 1 nm thick epilayer with a resulting dot diameter of ≈8 nm, a single luminescence peak with a maximum at 2.29 μm appears. The corresponding photon energy of 541 meV is blueshifted by 222 meV with respect to the 320 meV bandgap energy of bulk PbTe (vertical dotted line in figure 5). This blueshift due to quantum confinement is very close to that observed from chemically synthesized colloidal PbTe nanocrystals of the same size but with an organic shell [22]. In both cases, the linewidth is dominated by the size dispersion of the quantum dots.

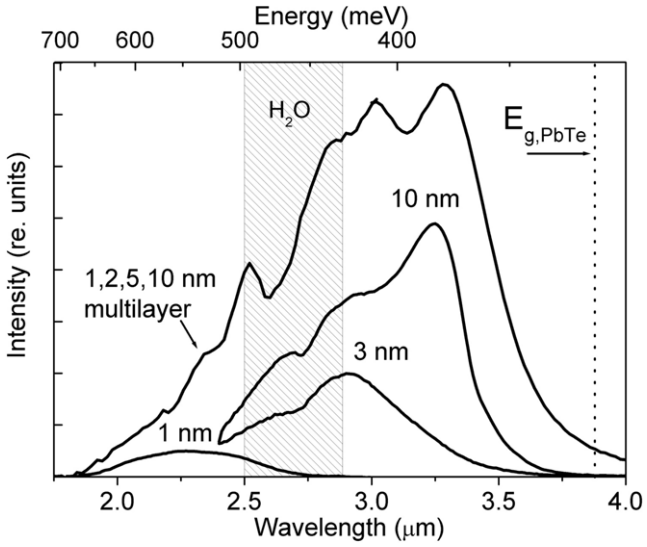

Figure 5. Room temperature photoluminescence spectra of PbTe/CdTe quantum dot precipitates obtained from annealed PbTe layers with thicknesses of 1, 3 and 10 nm, and for the multilayer sample. The shaded area indicates the region of an atmospheric water absorption band and the dashed vertical line indicates the bandgap energy of bulk PbTe.

Decreasing confinement due to increasing PbTe dot size leads to a rapid redshift of the luminescence signal. For instance, the dots formed from the 3 nm epilayer show their luminescence peak shifted to 2.91 μm due to the increased dot size of ≈15 nm (figure 5). The dots converted from the 10 nm layer yield two peaks at about 3.25 and 2.9 μm, where the former is attributed to emission from already fully developed quantum dots and the latter to residues of the original quantum well [20], which can also be seen in figure 2.

Due to the large overall dot size variation within the multilayer sample, an intense and very wide band luminescence emission is obtained over the whole 2.2–3.7 μm wavelength region (figure 5). This 1.5 μm broad emission band in combination with the high dot densities above 10^{11} cm^{-2} makes the studied material system attractive for the realization of superluminescent infrared light-emitting diodes [23], for which high output powers and large optical bandwidths are key figures of merit [24].

In conclusion, epitaxially controlled precipitation of coherent quantum dots from immiscible semiconductors is becoming a very promising and versatile self-organization scheme. In particular, we have investigated the fabrication of epitaxial PbTe quantum dots coherently embedded in a wide bandgap CdTe matrix. The size of the precipitates can be efficiently controlled via the initial thickness of the PbTe epilayer, which allows photoluminescence tuning over a very wide spectral region. Multilayers of dots with different diameters yields intense wide band mid-infrared emission, which should be particularly useful for superluminescence diodes in this spectral range.

Acknowledgments

This work was supported by the Austrian Science Fund, via projects SFB 025, START Y179 and P-17166.

References

[1] Bayer M *et al* 2001 *Science* **291** 451
[2] Ashoori R C 1996 *Nature* **379** 423
[3] Schedelbeck G *et al* 1997 *Science* **278** 1792
[4] Fafard S *et al* 1996 *Science* **274** 1350
[5] Arakava Y and Yariv A 1986 *IEEE J. Quantum Electron.* **22** 1887
[6] Yuan Z *et al* 2002 *Science* **295** 102
[7] Michler P *et al* 2000 *Science* **290** 2281
[8] Li X *et al* 2003 *Science* **301** 809
[9] Lundstrom T *et al* 1999 *Science* **286** 2312
[10] Kroutvar M *et al* 2004 *Nature* **432** 81
[11] Alivisatos A P 1996 *Science* **271** 933
Böberl M *et al* 2003 *Appl. Phys. Lett.* **82** 4065
Fürst J *et al* 2002 *Appl. Phys. Lett.* **81** 208
Springholz G *et al* 2001 *Appl. Phys. Lett.* **79** 1225
[12] Murray C B, Kagan C R and Bawendi M G 1995 *Science* **270** 1335
[13] Leonard D *et al* 1993 *Appl. Phys. Lett.* **63** 3203
Moison J M *et al* 1994 *Appl. Phys. Lett.* **64** 196
[14] Schukin V A and Bimberg D 1999 *Rev. Mod. Phys.* **71** 1125
[15] Stangl J, Holy V, Bauer G and Murray C B 2004 *Rev. Mod. Phys.* **76** 725 and references therein
[16] Palmstrom C J, Tabatabaic N and Allen S J 1988 *Appl. Phys. Lett.* **53** 2608
[17] Klenov D O, Driscoll D C, Gossard A C and Stemmer S 2005 *Appl. Phys. Lett.* **86** 111912
[18] Leute V, Haarmann N J and Schmidtke H M 1995 *Z. Phys. Chem.* **190** 253
[19] Koike K *et al* 2003 *J. Cryst. Growth* **247** 212
Koike K *et al* 2001 *J. Cryst. Growth* **227/228** 671
[20] Heiss W, Groiss H, Kaufmann E, Hesser G, Böberl M, Springholz G, Schäffler F, Koike K, Harada H and Yano M 2006 *Appl. Phys. Lett.* **88** 192109
[21] Leitsmann R, Ramos L E, Bechstedt F, Groiss H, Schäffler F, Heiss W, Koike K, Harada H and Yano M 2006 *New J. Phys.* **8** 317
[22] Urban J J, Talapin D V, Shevchenko E V and Murray C B 2006 *J. Am. Chem. Soc.* **128** 3248
[23] Ray S K, Groom K M, Alexander R, Kennedy K, Liu H Y, Hopkins M and Hoog R A 2006 *J. Appl. Phys.* **100** 103105
[24] Ngo C Y, Yoon S F, Fan W J and Chua S J 2007 *Appl. Phys. Lett.* **90** 113103